Bus selection index for distributed generators placement and sizing in the electrical network

Muhammad Raza, Aurangzeb Rashid Masud, Ayaz Hussain & Ravi Mohan Lal

Published online: 06 Oct 2022.

Submit your article to this journal ⬈

View related articles ⬈

View Crossmark data ⬈

Taylor & Francis
Taylor & Francis Group

REGULAR PAPER

Bus selection index for distributed generators placement and sizing in the electrical network

Muhammad Raza [a], Aurangzeb Rashid Masud [a], Ayaz Hussain[a] and Ravi Mohan Lal[b]

[a]Department of Electrical Engineering, Bahria University Karachi Campus, Karachi, Pakistan; [b]School of Science and Engineering, University of Dundee, Dundee, UK

ABSTRACT

Renewable energy sources, widely considered as distribution generation units, will be essential parts of the future electrical network. They will be integrated into the network at all voltage levels and act as the main controlling elements in the microgrid to stabilize the network. However, the objective of determining the suitable busbar to integrate the renewable generation source and its maximum capacity is still an indecisive problem. This article presents a methodology to select suitable busbars to integrate the renewable generation unit. A bus selection index is proposed based on three criteria, i.e. voltage deviation, active power loss, and grid energy infeed. The developed algorithm considers network busbar voltage limit and branch loading as constraints and the solution is determined using analytical technique. Algorithm is implemented in MATLAB, and MATPOWER is used for the power flow analysis. Furthermore, the proposed methodology is analysed on CIGRE and IEEE medium voltage benchmark network.

1. Introduction

Affordable and clean energy is one of the prime pillars of the United Nations (UN) sustainable development goals [1]. The importance of affordability with clean energy goals got precedence as the world economy and health system shattered with COVID-19 pandemic. According to UN statistics, one of four hospitals has no reliable electricity in the developing countries [1]. Traditional electrical network focus around centralized power generation, which produce more losses with increasing power flow and high voltage drops for longer transmission lines. Without significant reinforcement in the electrical transmission and distribution capacity, the consistently growing energy demand cannot be fulfilled even with the availability of large power plants. Alternatively, power generation system spread across the electrical network offer many benefits like energy generation where needed, lower losses, improved system stability, and convenient integration of renewable generation system [2]. Many countries such as Denmark and Germany are shifting from centralized to decentralized electrical structure using renewable energy sources as distributed power generation system [3].

Renewable sources have intermittent nature, and the renewable power plants (operating as distributed generation) posses small capacity which limit their capability to provide ancillary services such as reactive power support, frequency control, etc. [4]. Thus, distributed generation (DG) can significantly deteriorate the network performance if sited incorrectly and have an inappropriate size [5]. Distribution sources are placed and sized on the basis of certain technical and economical criteria such as minimizing the network active power losses, improving network voltage profile, reducing the energy import from the main grid, minimizing the investment cost, and maximizing profit [6,7]. Depending on the system study, either all or any one of these criteria can be applied for bus selection. However, usually, the economical criteria is applied for the selection of DGs among different types, i.e. wind turbine, PV system, fuel cells, biomass generator, energy storage system, and micro-hydro turbines, while the DG placement is based on the technical constraints.

Distribution generation units are usually integrated with low to medium voltage networks. The variation in the energy infeed by the DGs have high impact on the network operating conditions such as the impact of PV system on the rural and urban network is addressed in Ref. [8]. In Ref. [9], the optimum location of DG in the radial network is based on voltage stability, voltage deviation, and active power loss index. Similarly, in Refs. [10–16] the deployment of energy storage units and the analysis of PV systems effects on the network have been performed to determine the need of network reconfiguration. Static load model is usually applied when considering only DG output power variation for the analysis, but some researches have also considered the time-varying nature of the load [17–19].

CONTACT Muhammad Raza ✉ mraza.bukc@bahria.edu.pk

The problem of integrating DGs can be solved through analytical and optimization techniques. In analytical method, DG is connected to the network buses sequentially and power flow is calculated recursively over the range of DG active and reactive power. Results such as voltage deviation, active power loss, grid infeed and reactive power are recorded and compared to achieve the desired objectives without violating operating limits [9,20–26]. This technique is easy to implement for a small network but mathematical formulation for multiple objectives and result analysis become complex for large networks. On the other hand, optimization algorithms such as particle swarm method, ant colony, genetic algorithm, tabu search, etc. are also being used by the researchers for the DG placement and sizing [27–32]. In Refs. [33–35], the multi-objective optimization problem is formulated as mono-objective function in which the energy storage system and DG location is optimized according to their investment and network operational costs. In Ref. [7], a multi-objective optimization problem is formulated to select DG size according to total energy loss and maximizing DG generation profit. Literature shows that the mathematical and theoretical DG placement definition as optimization problem provides flexibility in implementing a large network, however, analysing the large solution data is complicated. Optimization results provide large data sets of voltages, power, and loading of the system for different scenarios that need to be analysed and compared for the bus selection and DG sizing. Large solution data problem is somewhat solved by defining evaluation indicator [36–38]. In Ref. [36], annual energy loss indication is formulated considering only DG active power. In Ref. [6], an optimal locator index is defined based on power loss sensitivity factor.

Optimum bus selection through evaluation indicator is relatively easy, however in existing literature, bus selection index is mostly based on single parameter only, such as energy loss index or voltage stability index or emission reduction, etc., and they cannot be modified easily to incorporate other criteria [13,30,39,40]. Furthermore, the DG sizing in the literature mainly address considering only DG active power. It is obvious that DGs can contribute to voltage support, thus it is important to analyse DG effect on its connected busbar as well as on all other busbars voltages individually with respect to reactive power infeed [3,4].

In this article, bus selection index for DG integration is proposed as a function of DG active and reactive power based on three sub-indices, i.e voltage index, grid power index, and power loss index. For better illustration, the contributions of the paper can be summarized as follows:

– A new methodology is proposed to formulate the indexes as non-conflicting objective function and they are based on the network performance criteria. This enables us to assess the network behaviour precisely.
– Since voltage is the primary parameter to be influenced by the integration of the DG, the voltage index is quantified by three aspects rather than considering only DG impact on average voltage of the whole network.
– A novel probabilistic-based penalty factor is introduced for busbars voltage and branches loading limits violation.
– The proposed index identifies the bus location and DG capacity for optimal network operation or maximum power integration.

Rest of the article is organized as follows: mathematical formulation of the three sub-indices is presented in Section 2. Then, the voltage and loading limits penalty factor is defined using probabilistic approach. In Section 3, an algorithm is presented to solve the DG integration problem with an analytical approach using selected indices. The proposed method is analysed on CIGRE and IEEE medium voltage benchmark by implementing algorithm in MATLAB using MATPOWER functions, and simulation results are discussed in Section 4. Finally some significant conclusions are drawn in Section 5.

2. Distribution generation placement and size criteria

Distribution generation sources of small capacity are usually integrated in low and medium voltage networks i.e below 50 MW. The selection of DG capacity and placement depends on both economical and technical feasibility. Economically, lower installation cost of DG with high energy penetration is desirable to maximize the profit. From technical feasibility perspective, the DG integration should not violate the voltage deviation limits, must not exceed the equipment thermal limits, and should not increase losses in the network. This article focuses only on technical parameters for the bus selection to integrate DG into the network. Primarily, the suitability of DG is determined through indexes of voltage, active losses, and grid power (either import or export). Furthermore, busbars operating voltages and branches (line, transformer, etc.) thermal loading limits are accounted as a penalty factor.

Consider a distribution network of Figure 1 having n number of busbars. The network configuration could be a radial or meshed, and the proposed bus selection methodology is applicable to both medium and low voltage networks. The network may consist of multiple feeding points from the national high voltage transmission grid, which is represented by the equivalent grid model. Grid provides power balancing for any
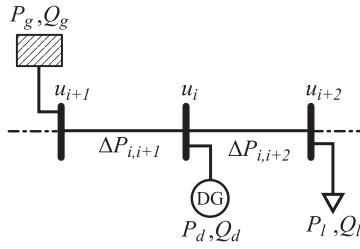
Figure 1. Distribution generation integration in the network.

mismatch between distribution generation and load. Distribution generation systems mainly feed energy into the grid through voltage source converter, which can control the active and reactive power independently [3,4]. Thus, DGs can be operated as either constant reactive power, power factor, or voltage magnitude control device. In this research, DG reactive power is controlled to maintain the constant power factor at the connected busbar. Power infeed by the distribution source changes the busbar voltages, varies the loading of the lines and transformers that consequently effects the losses, and influences the power infeed of the grid. Thus, the selection indexes are functions of DGs active and reactive power. A bus selection index (BSI) is introduced that depends on three indexes, i.e voltage index (VI), power loss index (PLI), and grid power index (GPI). These indexes are calculated for each busbar and compared for best location and size of the DGs. The indexes are formulated as minimizing function and can be applied in both analytical and optimization algorithm to select suitable busbar to integrate DG and its capacity determination.

The maximum number of DGs that can be connected in the grid is equal to the total number of busbars. However, the network planner can choose the desired number of DGs to be connected in the network. The total number of combination for DGs grid connection is calculated by using Equation (1).

$$ {}_nC_r = \frac{n!}{r!(n-r)!} = d \qquad (1) $$

Here, n is the total number of busbars, and r is the number of DGs that needs to be connected in the network. Further, each case of the combination gives the information of busbar at which DGs are connected. For calculating BSI of ith busbar, the combinations are divided into two sets, i.e A_i and B_i. The set A_i has the index of combination cases when at least one DG is connected to the ith busbar and the remaining indexes belong to the set B_i, thus A_i and B_i are disjoint sets.

Where,

$$ A_i : \{y_1, y_2, y_3, \ldots, y_w\} $$
$$ B_i : \{k_1, k_2, k_3, \ldots, k_{d-w}\} $$
$$ A_i \cup B_i : \{e_1, e_2, e_3, \ldots, e_d\} $$

2.1. Voltage index (VI)

The voltage index indicates the amount of change in the network voltages due to the addition of the DG. There are three aspects related to the voltage change i.e.

1. Change in the ith busbar voltage when DG is connected with it.
2. Average change in the network voltages (excluding ith busbar) when the DG is connected with ith busbar.
3. Average change in the ith busbar voltage when the DG is connected with other network busbars (excluding ith busbar).

Here, i is the index of a bus at which VI is calculated. The function ${}^af_i(u)$ is calculated using Equation (2) to analyse the sensitivity of the bus according to the power infeed by the DG. The rise and drop in the voltage magnitude based on the amount of reactive power infeed (either capacitive or inductive) while active power infeed usually raise the bus voltage. At this stage, it is insignificant to determine whether the voltages are improved or not rather the main objective is to identify the busbar at which maximum change in the voltage can be achieved.

$$ {}^a_y f_i(u) = \left| \frac{{}^y u_i - u_{i_0}}{u_{i_0}} \right| \quad i \in \mathbb{Z}^+, \ i \le n $$
$$ {}^a f_i(u) = \frac{1}{w} \sum_{y=1}^{w} {}^a_y f_i(u) \qquad (2) $$

where ${}^y u_i$ is the per unit voltage of the ith busbar with case index y, the index y is the combination when at least one DG is connected with ith bubar (A_i), w is the total number of combination elements of A_i, and u_{i_0} is the voltage at the ith busbar when DG is not connected to any busbar.

The objective of DG integration is not only to improve the voltage level of a single busbar but to make all busbars voltage level better. The average change in the network voltage is calculated using Equation (3).

$$ {}^b_y f_i(u) = \frac{\sum_{j=1}^{n} \left| \frac{{}^y u_j - u_{j_0}}{u_{j_0}} \right|}{n-1} \quad j \in \mathbb{Z}^+, \ j \neq i $$
$$ {}^b f_i(u) = \frac{1}{w} \sum_{y=1}^{w} {}^b_y f_i(u) \qquad (3) $$

Here, j is the index of network buses. ${}^y u_j$ is the voltage of jth busbar when DG is connected to ith busbar, and u_{j_0} is the voltage of jth busbar when no DG is connected.

Further, the possibility of improving the ith busbar voltage by connecting DG to other busbar is calculated

using Equation (4).

$$^c f_i(u) = \frac{\sum_{k=1}^{d-w} \left| \frac{k_{u_i} - k_{u_{i_0}}}{k_{u_{i_0}}} \right|}{d - w} \quad k \in \mathbb{Z}^+, \ k \in B_i \quad (4)$$

Here, the case index k is the combination when no DG is connected with the ith busbar (B_i). The effect of the DGs at ith busbar voltage is determined by combining $^a f_i(u)$, $^b f_i(u)$, and $^c f_i(u)$ as given by Equation (5).

$$f_i(u) = {}^a f_i(u) + {}^b f_i(u) - {}^c f_i(u) \quad (5)$$

High value of $^a f_i(u)$ and $^b f_i(u)$ indicate that the busbar is suitable for the placement of the DG. While higher value of $^c f_i(u)$ implies that the ith bus can be improved by placing DG on other buses, thus it lowers the DG placement suitability at ith bus.

The $f_i(u)$ is a maximizing function. To define voltage index (VI_i) as a minimizing function, $f_i(u)$ is multiple by -1 as given by Equation (6).

$$VI_i = -f_i(u) + |f_i(u) \cdot (2 - {}^u h_i - {}^{th} h_i)| \quad (6)$$

The power infeed by the DG may violate operating limits of busbars voltage and branches thermal loading. These limits are applied as penalty factors defined by $^u h_i$ and $^{th} h_i$, as explained in later section.

2.2. Power loss index (PLI)

The integration of DGs also reduces the losses in the network. The function $r_i(p)$ in Equation (7) determines change in the network active power loss at ith busbar compared to network losses without DG integration.

$$r_i(p) = \frac{1}{w} \sum_{y=1}^{w} \left(\frac{{}^y Ploss_i - Ploss_{i_0}}{Ploss_{i_0}} \right) \quad (7)$$

Here, $Ploss_{i_0}$ is the network total active power loss when no DG is connected, and $^y Ploss_i$ is the net active power loss of the network considering combination cases from set A_i. The negative value of $r_i(p)$ indicates that the losses have been reduced, thus power loss index as a minimizing function with penalty factor can be defined as Equation (8).

$$PLI_i = r_i(p) + |r_i(p) \cdot (2 - {}^u h_i - {}^{th} h_i)| \quad (8)$$

2.3. Grid power index (GPI)

Distribution sources support the local energy management system and reduce the reliance on feeding grid. The power generation in the distribution network increases the revenue by feeding the power into the high voltage grid. Further, DGs provide reactive power support to the network as well. The function $g_i(p, q)$

indicates the reduction in active and reactive power infeed by the HV substation.

$$g_i(p, q) = \frac{1}{w} \sum_{y=1}^{w} \left(\frac{{}^y p_i - p_{i_0}}{p_{i_0}} + \frac{{}^y q_i - q_{i_0}}{q_{i_0}} \right) \quad (9)$$

Here, p_{i_0}, and q_{i_0} are the active and reactive power of the grid without DG, whereas $^y p_i$, and $^y q_i$ are the active and reactive power considering combination cases from set A_i. The grid power index minimizing function with penalty factor is expressed by Equation (10).

$$GPI_i = g_i(p, q) + |g_i(p, q) \cdot (2 - {}^u h_i - {}^{th} h_i)| \quad (10)$$

2.4. Network operational limits

The energy infeed by the DG's changes the thermal loading of the branches (cables and transformers) and voltage level of busbars. These changes must not violate the network operational limits. Any violation in the network operational limits is considered as penalty factor, which reduces the suitability of a busbar as a potential candidate for connecting DG. Penalty factors are calculated as a cumulative normal distribution function. Using the cumulative distribution function, the probability that the busbars and branches are having values less than or equal to the operational limits is determined.

Two penalty factors are defined i.e $^u h_i$ and $^{th} h_i$ which indicates the violation of the voltage and thermal loading limits violation, respectively. To obtain the value of $^u h_i$, absolute change in the bus voltage from the rated value of all network busbars is calculated using Equation (11) for the combination cases of set A_i.

$$\Delta \, ^y u_j^{rt} = |^y u_j - 1.0| \quad j \in \mathbb{Z}^+ : j \le n \quad (11)$$

Here, j is the index of network buses and n is the total number of network buses.

Bus voltage varies with the infeed of the DG power. There might be some buses in the network which are operating below the operational limits before adding DG power but their voltages get improved afterward. Similarly, there could be some buses that may violate the limits after the addition of the DG power. Limit violation can be identified by comparing $\Delta \, ^y u_j^{rt}$ with the threshold value. Using Equation (11), the suitability of connecting DG at a busbar can be compared with others considering the number of violating buses and voltage magnitude deviation from the rated value. However, this information would be complicated to comprehend for a large network. Thus, the normal distribution can be applied on the data acquired using Equation (11) to determine the cumulative probability for a given value. This given value would be the limit value. The cumulative distribution function (CDF) determines the probability of the network voltages being less than or equal

to the limits. The CDF will approach zero when busbars violate the operational limit, while the CDF value 1.0 shows that no busbar is violating the voltage limit. The average, standard deviation, and CDF equations are defined as Equation (12).

$$
{}^{u}\mu_i = \frac{1}{w} \sum_{y=1}^{w} \frac{1}{n} \sum_{j=1}^{n} \Delta\, {}^{y}u_j^{rt}
$$

$$
{}^{u}\sigma_i = \frac{1}{w} \sum_{y=1}^{w} \sqrt{\frac{1}{n} \sum_{j=1}^{n} (\Delta\, {}^{y}u_j^{rt} - {}^{u}\mu_i)^2}
$$

$$
{}^{u}h_i = \frac{1}{{}^{u}\sigma_i\sqrt{2\pi}} \int_0^{u_{\lim}} \exp\left(-\frac{1}{2}\left(\frac{u - {}^{u}\mu_i}{{}^{u}\sigma_i}\right)^2\right) \mathrm{d}u
$$

$$(12)$$

The operational limit is applied on the absolute voltage deviation from the rated value because the busbars must not violate both the upper and lower limits. Here, the magnitude of the deviation is more important rather than the direction of the change i.e. either rise or drop from the rated value. Since the deviation value varies from zero to positive real number, the lower integral limit in the CDF can be set to zero and the upper limit would be the voltage operational limit. Typically, voltage deviation limit is ±10% in MV and LV distribution network thus, $u_{\lim}$ would be 0.1 p.u. Furthermore, thermal loading of the series elements such as cables and transformer is calculated using Equation (13) for combination cases from set A_i.

$$
\Delta\, {}^{y}I_l^{rt} = \frac{{}^{y}I_l}{I_l^{rt}} \tag{13}
$$

Here, l is the index of the element, I_l^{rt} is the element rated current value in ampere, and ${}^{y}I_l$ is the magnitude of actual current flowing through l element in ampere.

Similarly, CDF is calculated to apply thermal limit. The average, standard deviation, and CDF equations are defined as Equation (14) for calculating the probability of elements operating below thermal limit. Generally, all elements loading must not exceed 100% thus the thermal limit $i_{\lim}$ would be 1.0 p.u. Also, CDF value 1.0 shows that no element has violated the thermal loading limit. The value of the element loading varies from zero to positive real number, thus the lower limit in CDF equation is set to zero.

$$
{}^{th}\mu_i = \frac{1}{w} \sum_{y=1}^{w} \frac{1}{m} \sum_{l=1}^{m} \Delta\, {}^{y}I_l^{rt}
$$

$$
{}^{th}\sigma_i = \frac{1}{w} \sum_{y=1}^{w} \sqrt{\frac{1}{m} \sum_{l=1}^{m} (\Delta\, {}^{y}I_l^{rt} - {}^{th}\mu_i)^2}
$$

$$
{}^{th}h_i = \frac{1}{{}^{th}\sigma_i\sqrt{2\pi}} \int_0^{i_{\lim}} \exp\left(-\frac{1}{2}\left(\frac{I - {}^{th}\mu_i}{{}^{th}\sigma_i}\right)^2\right) \mathrm{d}I
$$

$$(14)$$

Moreover, the probability that network busbars and series branch elements will have voltages and thermal loading above the operational limits can be calculated using Equation (15).

$$
P(X > u_{\lim}) = 1 - {}^{u}h_i \quad \because X = \Delta\, {}^{y}u_j^{rt}
$$

$$
P(Y > i_{\lim}) = 1 - {}^{th}h_i \quad \because Y = \Delta\, {}^{y}I_l^{rt} \tag{15}
$$

These two probabilities are mutually exclusive and added together to be applied as a factor of index. For example, if $f(z)$ is a minimizing function than the best result would be at its least value. However, the solution would not be suitable if at this least value there exists any violation of operational limit. So, $f(z)$ is increased in a positive direction as a factor of the operational limits violation probabilities to worsen its value. Mathematically, it can be expressed as Equation (16).

$$
\hat{f}(z) = f(z) + |f(z) \cdot (2 - {}^{u}h_i - {}^{th}h_i)| \tag{16}
$$

For no violation situation, the value of ${}^{u}h_i = {}^{th}h_i = 1.0$ and the last term of above equation becomes zero hereby no penalty factor is applied.

2.5. Bus selection index (BSI)

Bus selection index of ith busbar is defined as Equation (17). Any network busbar having the least value of BSI would be the best candidate for integrating the DG.

$$
BSI_i = VI_i + PLI_i + GPI_i \tag{17}
$$

The proposed selection index can be used to find more than one suitable busbar by ranking them in ascending order based on their BSI value. If more than one busbars have the same BSI then the decision can be made based on either observing the power to be feed-in by DGs (maximum would be preferable), or based on the individual index. The developers can decide if they prefer more voltage to be improved or give priority to losses.

2.6. Performance index (PI)

The performance index indicates the probability of the busbar or the series branch element of violating the network operational limit while connecting DG at all network busbars. This is expressed by two variables, i.e ${}^{u}h_i^{rt}$, and ${}^{th}h_l^{rt}$. To calculate performance index at the busbars, an absolute voltage deviation of the ith busbar voltage from the rated value is calculated using Equation (18) for all combination cases.

$$
\Delta\, {}^{e}u_i^{rt} = |\, {}^{e}u_i - 1.0| \quad e \in (A_i \cup B_i) \tag{18}
$$

Here, i is the busbar at which performance is calculated, and e is the index of all combination cases. The mean, standard deviation, and CDF equation of ith busbar

voltage is calculated using Equation (19). The voltage operation limits (u_{lim}) are also set here as 0.1 p.u.

$$^u\mu_i^{rt} = \frac{1}{d}\sum_{e=1}^{d}\Delta\,^e u_i^{rt}$$

$$^u\sigma_i^{rt} = \sqrt{\frac{1}{d}\sum_{e=1}^{d}(\Delta\,^e u_i^{rt} - \,^u\mu_i^{rt})^2}$$

$$^u h_i^{rt} = \frac{1}{^u\sigma_i^{rt}\sqrt{2\pi}}\int_0^{u_{lim}}\exp\left(-\frac{1}{2}\left(\frac{u - \,^u\mu_i^{rt}}{^u\sigma_i^{rt}}\right)^2\right)du$$

(19)

Similarly, loading of the *l*th series branch element is calculated for all combination cases.

$$\Delta\,^e I_l^{rt} = \frac{^e I_l}{I_l^{rt}}$$

(20)

The probability of the series branch element of violating the thermal limits is calculated using Equation (21). The thermal limit i_{lim} is equal to 1.0 p.u.

$$^{th}\mu_l^{rt} = \frac{1}{d}\sum_{e=1}^{d}\Delta\,^e I_l^{rt}$$

$$^{th}\sigma_l^{rt} = \sqrt{\frac{1}{d}\sum_{e=1}^{d}(\Delta\,^e I_l^{rt} - \,^{th}\mu_l^{rt})^2}$$

$$^{th}h_l^{rt} = \frac{1}{^{th}\sigma_l^{rt}\sqrt{2\pi}}\int_0^{i_{lim}}\exp\left(-\frac{1}{2}\left(\frac{I - \,^{th}\mu_l^{rt}}{^{th}\sigma_i^{rt}}\right)^2\right)dI$$

(21)

3. Implementation of bus selection index in analytical technique

The proposed distribution source integration methodology is based on the analytical technique and determines the suitable busbar location according to the network capability. The presented algorithm identifies the DG active power at which network will operate in the most optimized manner. The solution also indicates the maximum capacity of the DG that can be infeed into the network considering network constraints. Furthermore, the proposed method is applicable for both single or multiple DGs integration. Following are the steps which algorithm performs to acquire the desired results:

- *Step 1*: The network model is built in the MATPOWER to perform the power flow computation. Distribution generation unit is modelled as a constant PQ source.
- *Step 2*: Active power range of distribution generation unit is set from zero to estimated maximum power that can be feed into the network. Any arbitrary value can be set for the maximum power, however, it

is to be ensured that the power flow should converge at all active power set-points.
- *Step 3*: At least 100 steps change in the DG output power between minimum and maximum values are defined to acquire the sufficient number of sample data. However, this step size can be varied considering the algorithm computation time. The step change in active power can be calculated as $(P_{d\_max} - P_{d\_min})/$No. of Sample required.
- *Step 4*: The DG reactive power capability is set to 0.9 power factor (capacitive and/or inductive) to fulfill the minimum requirement set by grid operators.
- *Step 5*: 10% bus voltage magnitude limit and 100% branches loading limit are set as network constraints.
- *Step 6*: Power flow calculation is performed without DG connection at any bus and results are recorded.
- *Step 7*: Define the maximum number of DGs required to be connected with the grid. DGs are connected at all busbar according to the combinations as defined by Equation (1). Power flow calculation is performed over the range of DG output active power as defined in step 2. Results are recorded.
- *Step 8*: Step 6 and 7 is performed for DG output power at 0.9 capacitive, 0.9 inductive, and 1.0 power factor.
- *Step 9*: VI, PLI, GPI, and BSI are calculated for all network buses.
- *Step 10*: Busbar and branches are identified for any violation. Furthermore, performance index are calculated to determine the network elements probability of deviating from rated value.

4. Network analysis and simulation results

The proposed bus selection index is implemented and analysed on the CIGRE medium voltage benchmark network and IEEE 33 bus benchmark network considering both single DG integration as well as integrating multiple DG simultaneously. The algorithm is implemented in MATLAB using MATPOWER functions. The loads are considered constant at their most probable values for the power flow analysis, and generator-oriented sign convention is used in the power flow results.

4.1. DG integration analysis on CIGRE network

The CIGRE medium voltage benchmark network is shown in Figure 2 and the network parameters are taken from Ref. [41]. The network is modelled as meshed network and the power flow calculation without any DG in the network shows that the minimum busbar voltage would be 0.95 p.u. The transformers (Br1 and Br2) have the maximum loading i.e 72%. The active power loss is 0.109 MW and the reactive power demand of the network branches is
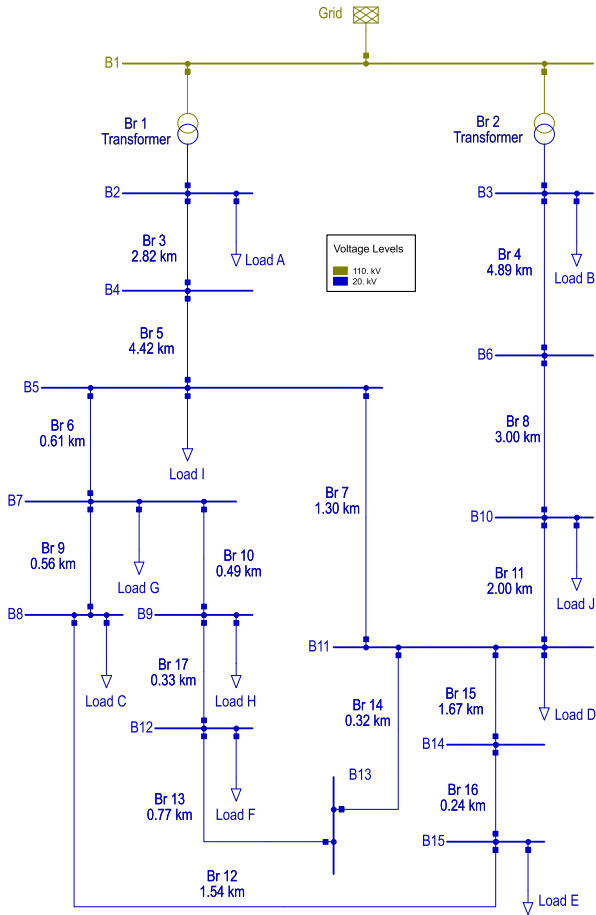
Figure 2. CIGRE MV benchmark network.

Figure 3. Bus selection index at 0.9 capacitive power factor.

Figure 4. Comparison of bus selection index at 15 MW DG infeed power considering different power factors.

Figure 5. Individual index at 15 MW DG infeed power with 1.0 power factor.

3.19 MVar. Moreover, the 'Grid' supplies the total power of 34.29 MW and 7.14 MVar to fulfil the network load demand.

The response without DG indicates that the busbar voltages are lower than the rated values and network demands capacitive reactive power. Thus, bus selection index is calculated for the active power range from 0.0 to 20 MW at 0.9 capacitive power factor as shown in Figure 3. The most suitable bus for the DG integration is at the lowest BSI value at any given DG active power. Although bus 'B1', 'B2', and 'B3' appears suitable for high DG active power output, the network would not operate efficiently which means the network voltages and loading are not improved and their values are closed to 'no DG' response. DG placement other than 'B1', 'B2', 'B3' at high power would worsen the network response as the losses in the network will increase significantly. The average increase in the total network losses would be up to 0.65 MW at 15.0 MW DG active power infeed. The positive sign of the BSI index indicates that the network response becomes worse compared to without DG connected condition as shown in Figure 4. Figure 4 shows that the network cannot be improved despite providing reactive power support by the DG. Furthermore, DG needs to be operated near 1.0 power factor at 15.0 MW DG output power. The individual index, as shown in Figure 5, indicates
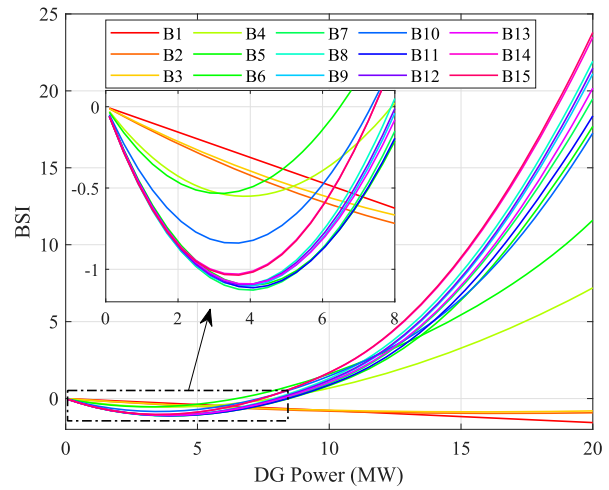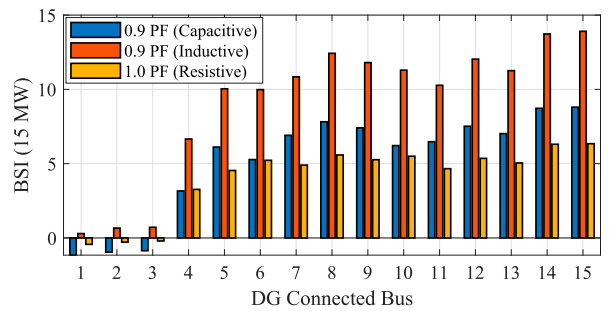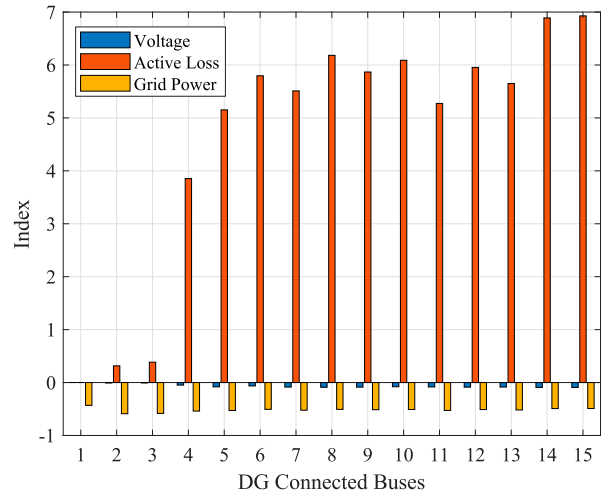
that the active power losses are increased significantly regardless at which busbar DG is connected, and the improvement in the bus voltages and energy infeed into the grid is minimum.

The maximum DG active power output is limited by the constraints of the network. The response of at least one busbar voltage limit violation is shown in Figure 6. Similarly, Figure 7 shows the response of at least one branch loading limit violation. The responses
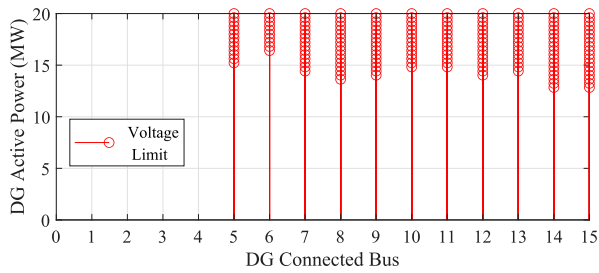
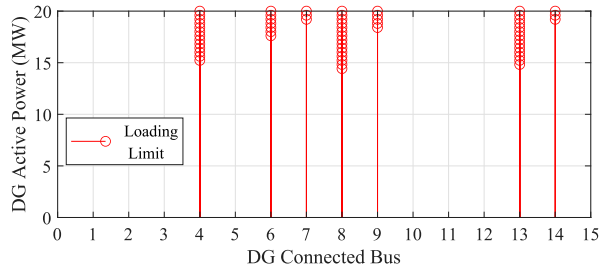**Figure 6.** Voltage limit violation at 0.9 capacitive power factor.

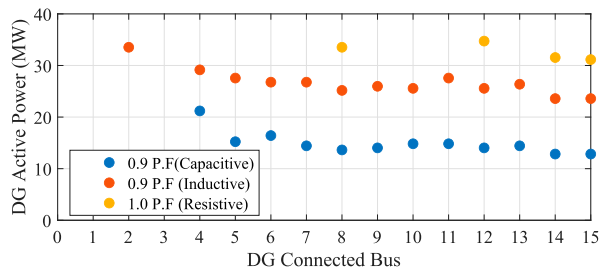**Figure 7.** Branch loading limit violation at 0.9 capacitive power factor.

Figure 8. At least one busbar voltage limit violation comparison at different power factors.

Figure 9. At least one branch loading limit violation comparison at different power factors.

Figure 10. BSI response of Bus 7 at different power factors.

Figure 11. Individual index comparison at DG power 4.0 MW and 0.9 capacitive power factor.

imply that the maximum output of the DG can only be 13 MW if connected to bus 'B15' since at least one busbar violate the limit. On the other hand, there will be no voltage limit violation up to 20 MW if DG is connected with the buses 'B1' to 'B4' ; however, branch loading limit will be violated at 'B4' for DG active power 15 MW and above. The maximum infeed power at different power factor can be determined by analysing Figures 8 and 9. The range of DG active power output is increased from 20 to 40 MW in the simulation. Although the active power infeed capability can be increased with respect to voltage limit by controlling DG reactive power, the loading of the branches cannot be improved significantly as shown in Figure 9. At bus 'B3' and 'B4' the loading of the transformer would be the main limiting factor and the DG power can be increased up to 32 MW, whereas DG connected at bus 'B1' (grid bus) provides no benefit in term of network voltages and active power losses improvement.

The minimum BSI is at 4.0 MW as shown in Figure 3. This is the most suitable DG active power infeed location to achieve the best-optimized network operation
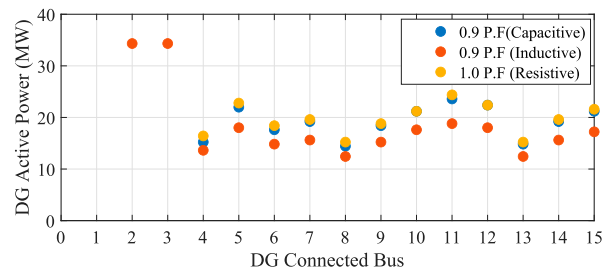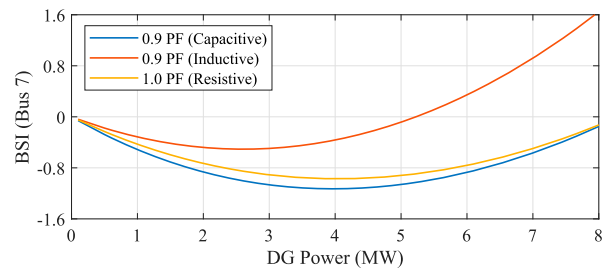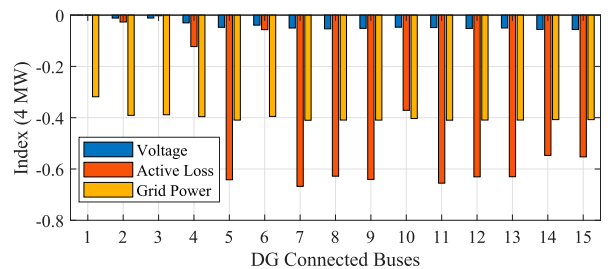
considering all three indexes. The buses can be ranked in ascending order for DG integration suitability. At 4.0 MW, the bus 'B7' is the most suitable candidate to integrate DG while 'B11' would be next suitable candidate.

The response of 'B7' BSI at different power factor is shown in Figure 10. The response shows that the DG needs to be operated with capacitive power factor in order to achieve optimized network operation while inductive power factor will deteriorate the network performance. The comparison of the voltage, active power loss, and grid power indexes at 4.0 MW DG power is shown in Figure 11. Primarily, active power loss improved significantly when DG is connected at 'B7'. Further it also enables the maximum energy transfer to the higher grid from the distribution generation unit. Although the voltage improvement rank of 'B7' is 4.0, its performance is comparable to the highest ranked bus ('B15'). The VI at 'B15' is −0.056 and VI at 'B7' is −0.050. The analysis concludes that the 'B7' is highest ranked busbar based on BSI and most suitable for integrating the DG.

In the above analysis, suitable busbar is determined for the placement and sizing of a single DG. Similarly, suitable location for multiple DGs integration can also be determined using the proposed methodology. The required number of DGs is the input parameter and it can be set up to the maximum number of busbars i.e 15 DGs on CIGRE network. However, for simplification, the bus selection index and sizing comparison analysis is performed up to 6 DGs integrated simultaneously. The minimum BSI of each busbar and the net active power feed by the DGs is shown in Figure 12. The plot shows the comparison of the busbars suitability for integrating multiple DGs simultaneously. In case of 2 DGs connecting in the grid, the most suitable bus to connect at least one DG is B3 and B2, and the net optimium power of the 2 DGs could be between 8.84 and 9.33 MW. Bus selection index at B2 and B3 is minimum since large DGs can be integrated on these buses compare to other busbars, consequently more energy can be feed into the grid. Similarly, improvement in the network voltages and losses increase with the increase in the number of DGs. With 6 DGs, network operational level will be improved significantly while connecting them on busbars from 4 to 15. Obviously, DGs connection at busbar 1 to 3 do not provide significant improvements in the network voltage and losses since they are close to the grid feeding point. The net optimium active power for 6 DGs integration is around 6.0 MW having each DGs approximately 1.0 MW of capacity. Furthermore, it is also evident that the size of the DGs integrated far from the grid feeding point having much greater power than nearby loads is not beneficial. In Figure 13 network busbar voltage limits are compared. The result indicates net DGs active power at which at least one busbar voltage violates limit while the corresponding busbar must be connected with a DG. For instance, considering the case of 5 DGs integration at busbar 11 to 15, the net DG power should be less then 15.0 MW while the maximum voltage violation at 15.0 MW would be 0.107 p.u i.e. 10.7%. Similarly, the thermal loading limit violation results with respect to the net DGs power is shown in Figure 14. Further in this case, the first branch loading violation would occur when the net DG power would exceed 20.0 MW, so in this case voltage violation parameter will be given priority for selecting the maximum size of the DG.

The algorithm is tested on the standard Intel (R) Core (TM) i9-10850K CPU@ 3.6 GHz based system. The execution time of the algorithm for multiple DGs integration analysis is shown in Table 1. Note that the total iteration does not include the power flow iteration, i.e Newton Raphson iteration. The algorithm provides a deterministic solution, having fast execution time, and covers wide range of DG power with sufficient step size.
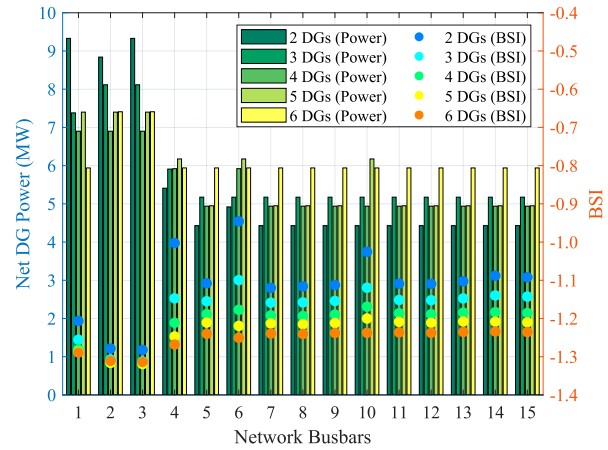
Figure 12. Comparison of BSI and sizing at each busbar for simultaneously connected DGs.
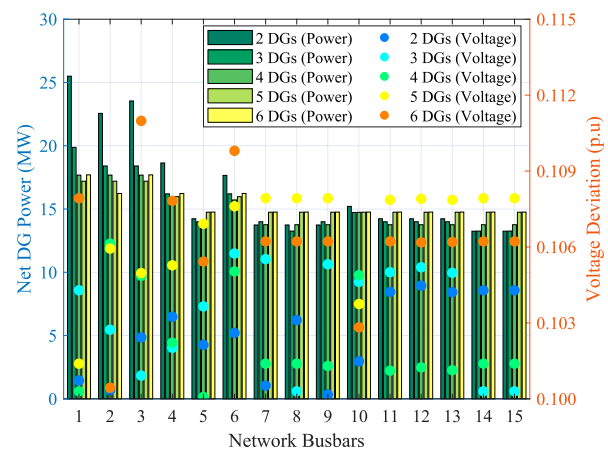
**Figure 13.** Comparison of at least one busbar voltage deviation for simultaneously connected DGs.
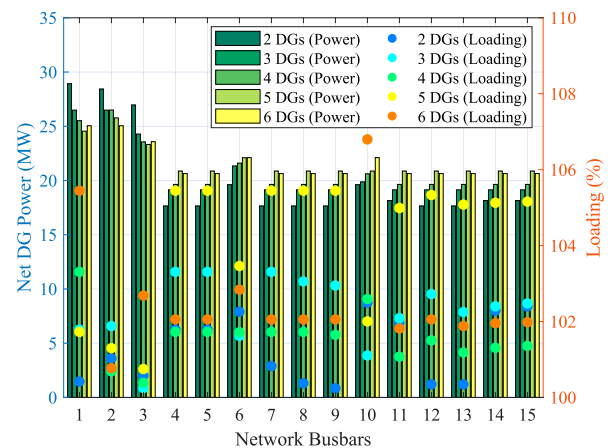
Figure 14. Comparison of at least one branch loading limit violation for simultaneously connected DGs.

4.2. DGs integration analysis on IEEE 33 bus network

The proposed methodology is also analysed on the IEEE medium voltage 33 bus standard network as given in Figure 15. The network is in radial configuration

Table 1. Computational time of the algorithm for a 15 bus CIGRE network.

No. of DGs	No. of step change in power	No. of cases	Total iteration	Execution time (s)
1	101	15	1515	1
2	101	105	10,605	12
3	101	455	45,955	53
4	101	1365	137,865	162
5	101	3003	303,303	371
6	101	5005	505,505	634
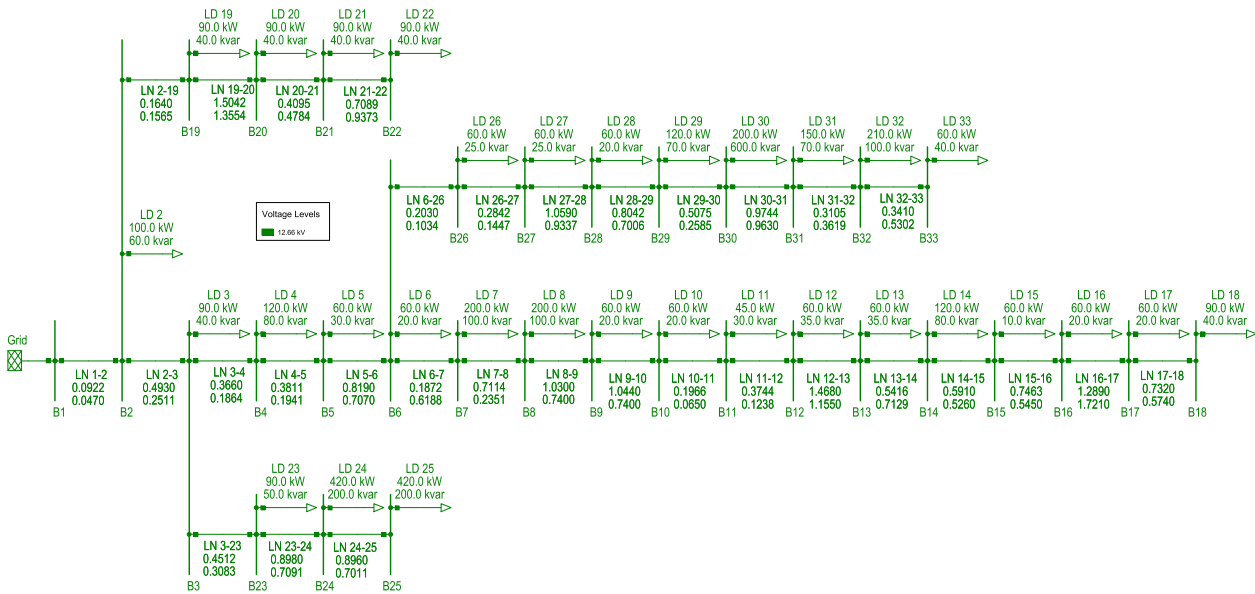
Figure 15. IEEE medium voltage 33 bus standard network.

having 12.66 kV voltage level, and the parameters are taken from Ref. [42]. The cables resistance and reactance values in Ohms are given in the diagram, respectively. Also, the current carrying capability of the cables are sets as 0.3 kA. All the loads have lagging power factor. It is obvious that the capacitive reactive power infeed by the DGs would improve the network voltages. Thus, the DG power factor is set as 0.90 leading to acquire the maximum voltage support. The analysis has been performed to integrate multiple DGs simultaneously and determines the suitable busbars and the DG power.

Without any DG integration, the grid is required to supply the energy of 3.92 MW and 2.44 MVar. The maximum voltage drop is at B18 having 0.913 p.u voltage level. The total active power loss of the network is 0.203 MW and the network cables requires 0.14 MVar inductive power. Further, the maximum active power loss occur in cable 'LN 2-3' i.e 0.05 MW.

Bus selection index up to 3 DG integration is shown in Figure 16. It can be observed that the most suitable bus for single DG integration is B2 and the size of the DG is 10.0 MW. B2 BSI is −4.3806 and the second suitable bus is B1 with −4.3037 BSI. Figure 16 shows the minimum BSI possible at each busbar with respective DG size while Figures 17 and 18 show at least one limit violation of branch loading and busbar voltage magnitude. By comparing the limit violation

plots with the BSI, it can be observed that the loading of the branches are violated at the lower DG size. For example, the BSI of B1, B2, and B19 is −3.276, −3.188 and −3.233, respectively, for 3 DGs simultaneously integration. These BSI are achieved with net DG size of 7.822 MW while the loading limits is violated at 9.9201 MW for B1 & B2, and 6.6234 MW B19. Similarly, the busbar voltage limits is violated at 3.3267 MW while connecting DGs at B1, B2, and B19 thus the DGs with net active power of 7.822 MW cannot be connected due to voltage limit violation. In this case, the net active power of 3 DGs should be less than 3.3267 MW. It is to be noted that the BSI is lowest despite the operational limit violation, this implies that the network performance could be improved outside its boundary limits. The solution shown in Figure 17 said to be a global optimum point while BSI and DGs net active power values defined by the voltage and loading limits are local minima. The BSI value at net DGs active power values based on voltage limits is shown in Figure 19. Considering the local minima point, B1 is suitable for single DG integration, B3 and B23 are the most suitable busbar for 2 DGs simultaneous integration, and B23, B24, and B25 are suitable for 3 DGs simultaneous integration.

As mentioned previously, the BSI is based on three index and the indexes are the indicators of how much a voltage level and active power losses in the network
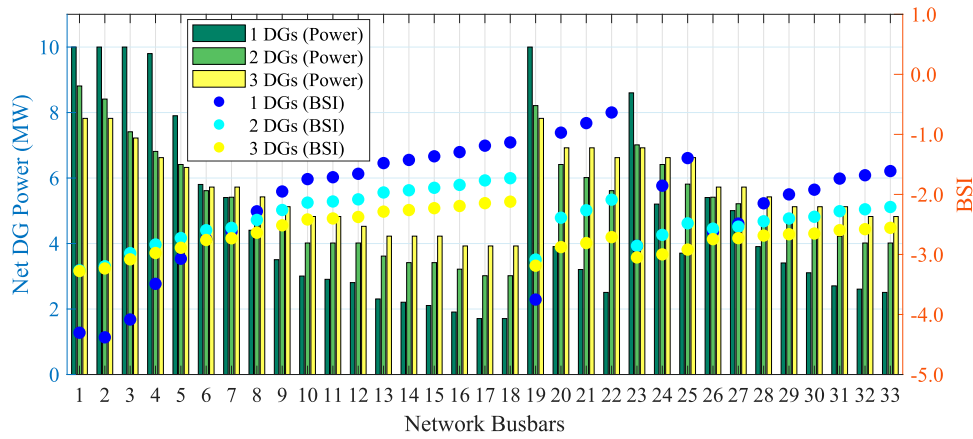
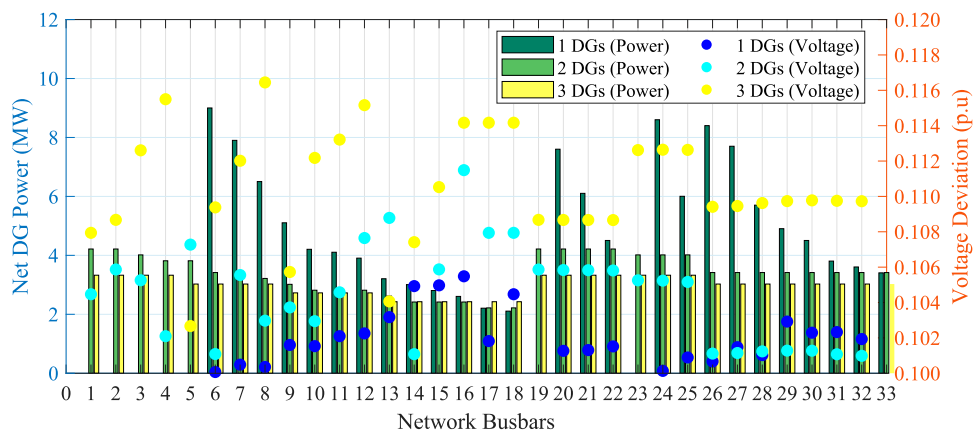**Figure 16.** Bus selection index of IEEE medium voltage 33 bus standard network for integrating multiple DGs.

Figure 17. Comparison of branches loading limit violation on IEEE medium voltage 33 standard network.
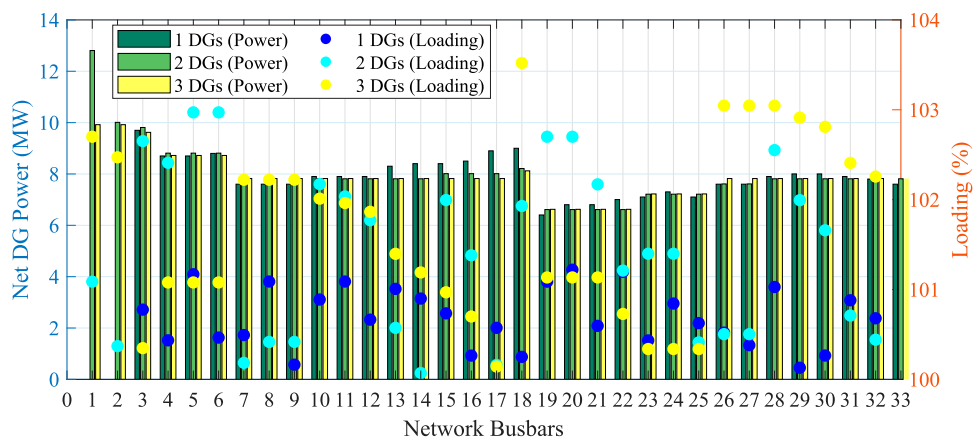

Figure 18. Comparison of voltage limit violation on IEEE medium voltage 33 standard network integrating multiple DGs.

can be improved as well as the energy that can be feed-in by DGs into the grid after fulfilling the network load demands. These indexes are non-conflicting in nature; however, the improvement in the each index varies location-to-location. In certain case, one index might be improving but others don't. This usually occurs at the global optimum point since it is disregarding the operational limits. For example, the global optimum point at B19 for single DGs placement is −3.75153 (BSI) as given in Figure 16 while VI is −0.0331, PLI is equal to 1.688, and GPI value is −6.10647. It is clear that the active power losses in the network have

been increased due to reverse energy flow while voltage level is improved and more energy is feed into the upper-level grid.

It is also important to determine the global optimum point of each individual index. This would help to determine how much the individual indexes can be improved in the network. The results shown in Figures 20–22 quantify this analysis. For single DG placement, the most suitable busbar from voltage improvement perspective is B18 having VI value −0.2758 and the size of the DG would be 3.7063 MW. The second most suitable busbar would B33 with −0.2626 VI value
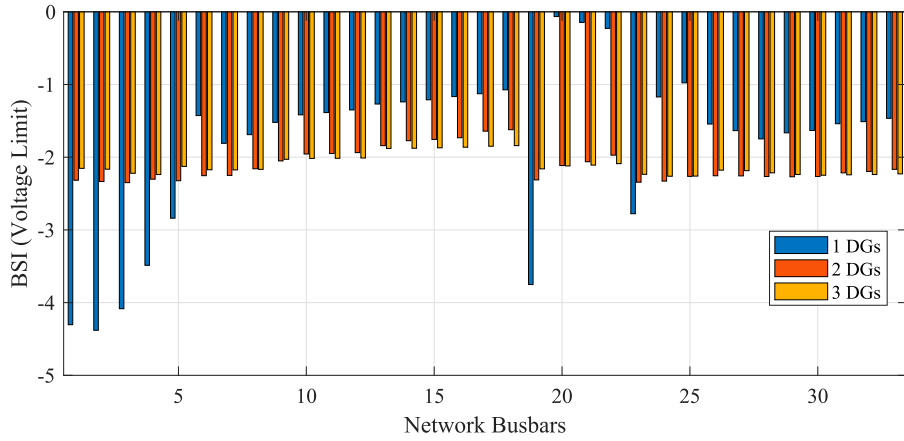
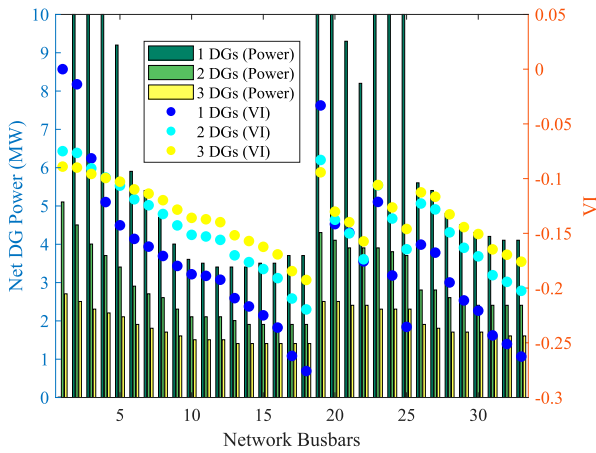**Figure 19.** BSI values at busbar voltage violation limit for IEEE medium voltage 33 standard network.

Figure 20. Optimum VI values at each busbar of IEEE medium voltage 33 standard network.

Figure 21. Optimum PLI values at each busbar of IEEE medium voltage 33 standard network.
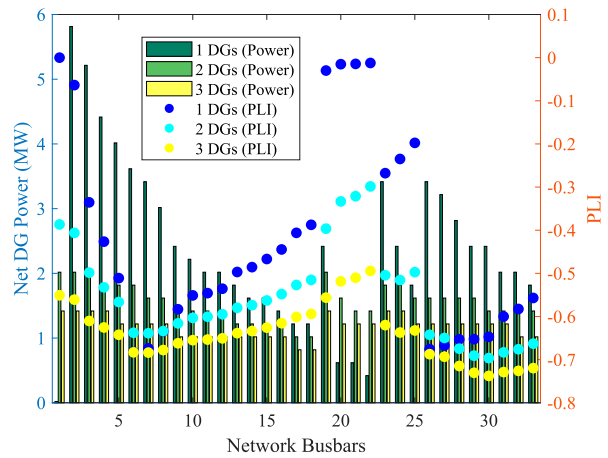

Figure 22. Optimum GPI values at each busbar of IEEE medium voltage 33 standard network.

and 4.106 MW DG active power. For 2 DGs simultaneous integration, B17 and B18 are most suitable and DGs with net active power of 1.9081 MW can be connected i.e 0.9540 MW each. For 3 DGs simultaneous integration, B17, B18, and B33 are suitable with net active power of 1.47 MW, i.e. approximately 0.5 MW each. It can be observed that the size of an individual DGs is reduced with the increase in the number of the DGs connected simultaneously, and the improvement in the network voltage would be lower.

Similarly, the suitable busbar from active power loss improvement perspective is B26 for single DG integration having PLI −0.6756 with 3.416 MW capacity. B29 and B30 are suitable for 2 DGs integration having net DG capacity of 1.5185 MW i.e. 0.76 MW each. For 3 DGs integration, busbars B29, B30, and B31 are suitable having PLI value of −0.7301, −0.738, and −0.728, respectively. The optimum net DG power is 1.2188 MW. The analysis indicates that more distributed generations are suitable for improving the network active power losses. Furthermore, the DGs integration near to the feeder is suitable to maximize profit by feeding the energy back to the higher voltage level

grid which is evident from Figure 22 that B1 and B2 are suitable for multiple DGs integration.

The proposed algorithm provides the deterministic solution and has the ability to analyse both global and local optimum points with fast execution time. The execution time of algorithm for the IEEE 33 bus medium voltage standard network is given in Table 2. The total

Table 2. Computational time of the algorithm for a 33 bus IEEE network.

No. of DGs	No. of step change in power	No. of cases	Total iteration	Execution time (s)
1	101	33	3333	4.1
2	101	528	53,328	65.29
3	101	5456	551,056	695.2

number of iteration for single DG placement is 3333, which is executed in approx 4.1 s. Also, the execution time is fast for 2 and 3 DGs simultaneous placement, i.e 65.29 and 695.2 s, respectively.

5. Conclusion

The proposed bus selection methodology caters multiple performance parameters for the selection of suitable busbar to integrate multiple DGs with medium voltage network. The solution provides the maximum power that a DG can infeed into the grid and the power at which network will operate in most optimized manner. The analysis shows that the global optimum point could exist outside the boundary limits, and the network can be operated at this global point by making operational limits less strict. In certain cases, global optimum point exists outside the boundary limits in multi-objective index when one or more index is maximizing while others are minimizing. Further, the analysis shows that more number of DGs in the network are suitable in all the cases. Such as, one DG provides more optimized operation for network voltage improvement perspective and should be connected far from the feeders. While, more number of DGs distributed in the network are suitable to improve the network losses however the size of the DGs would be small. On the other hand, DG of larger size should be connected near to the feeders to be able to feed energy into upstream network with ease. Furthermore, the utilization of converter in distribution system enables the control of both active and reactive powers thus the need of static VAR compensator is reduced and the reactive power compensation can be done through DGs. Therefore, DG sizing has been done in the proposed algorithm considering both active and reactive powers. It is obvious that the DG size is limited by the network operational limits, however, the suitability of a busbar must be analysed considering the number of network elements that are approaching the limit value. If more number of network elements approach limit value, the busbar becomes less suitable. This methodology is implemented by introducing probabilistic-based penalty factor. Although the proposed index is implemented through analytical technique, the index can also be implemented as optimization problem. The future extension of this work would be to implement the proposed bus selection index as optimization problem considering the stochastic nature

of the load and DG input power for simultaneously integrating multiple DGs in the network.

Disclosure statement

No potential conflict of interest was reported by the author(s).

ORCID

Muhammad Raza http://orcid.org/0000-0002-4385-5020
Aurangzeb Rashid Masud http://orcid.org/0000-0001-5225-2662

References

[1] Jensen L. The sustainable development goals report 2020. New York (NY): United Nation; 2020. (Tech. Rep.).
[2] Adefarati T, Bansal R. Integration of renewable distributed generators into the distribution system: a review. IET Renew Power Gener. 2016 Aug;10(7):873–884.
[3] Blaabjerg F, Yang Y, Yang D, et al. Distributed power-generation systems and protection. Proc IEEE. 2017 Jul;105(7):1311–1331.
[4] Olek B, Wierzbowski M. Local energy balancing and ancillary services in low-voltage networks with distributed generation, energy storage, and active loads. IEEE Trans Ind Electron. 2015 Apr;62(4):2499–2508.
[5] Galvan E, Mandal P, Haque AU, et al. Optimal placement of intermittent renewable energy resources and energy storage system in smart power distribution networks. Electr Power Compon Syst. 2017 Aug;45(14):1543–1553.
[6] Lee SH, Park JW. Optimal placement and sizing of multiple DGs in a practical distribution system by considering power loss. IEEE Trans Ind Appl. 2013;49(5):2262–2270.
[7] Radosavljevic J, Arsic N, Milovanovic M, et al. Optimal placement and sizing of renewable distributed generation using hybrid metaheuristic algorithm. J Mod Power Syst Clean Energy. 2020;8(3):499–510.
[8] Hernández JC, Medina A, Jurado F. Impact comparison of PV system integration into rural and urban feeders. Energy Convers Manag. 2008;49(6):1747–1765.
[9] M'hamdi B, Teguar M, Tahar B. Optimal DG unit placement and sizing in radial distribution network for power loss minimization and voltage stability enhancement. Period Polytech Electr Eng Comput Sci. 2020 Jan;64(2):157–169.
[10] Santos SF, Fitiwi DZ, Cruz MR, et al. Impacts of optimal energy storage deployment and network reconfiguration on renewable integration level in distribution systems. Appl Energy. 2017 Jan;185:44–55.
[11] Emmanuel M, Rayudu R. The impact of single-phase grid-connected distributed photovoltaic systems on the distribution network using P-Q and P-V models. Int J Electr Power Energy Syst. 2017 Oct;91:20–33.
[12] Watson JD, Watson NR, Santos-Martin D, et al. Impact of solar photovoltaics on the low-voltage distribution network in New Zealand. IET Gener Transm Distrib. 2016 Jan;10(1):1–9.
[13] Reza M, Schavemaker P, Slootweg J, et al. Impacts of distributed generation penetration levels on power systems transient stability. In: IEEE Power Engineering Society General Meeting, 2004. Vol. 2. IEEE; 2004. p. 2151–2156.

[14] Elphick S, Drury G, Fixter B. The impact of small scale solar PV on power quality: an empirical study. In: 2020 19th International Conference on Harmonics and Quality of Power (ICHQP); 2020 Jul. IEEE. 2020. p. 1–6.

[15] Al Momani T, Harb A, Amoura F. Impact of photovoltaic systems on voltage profile and power losses of distribution networks in Jordan. In: 2017 8th International Renewable Energy Congress (IREC). IEEE; 2017 Mar. p. 1–6.

[16] Baghban-Novin S, Mahzouni-Sani M, Hamidi A, et al. Investigating the impacts of feeder reforming and distributed generation on reactive power demand of distribution networks. Sustain Energy Grids Netw. 2020 Jun;22:100350.

[17] Zhu D, Broadwater RP, Tam KS, et al. Impact of DG placement on reliability and efficiency with time-varying loads. IEEE Trans Power Syst. 2006 Feb;21(1):419–427.

[18] Essallah S, Khedher A, Bouallegue A. Integration of distributed generation in electrical grid: optimal placement and sizing under different load conditions. Comput Electr Eng. 2019 Oct;79:106461.

[19] Hung DQ, Mithulananthan N, Lee KY. Determining PV penetration for distribution systems with time-varying load models. IEEE Trans Power Syst. 2014 Nov;29(6):3048–3057.

[20] Zhang C, Li J, Zhang YJ, et al. Optimal location planning of renewable distributed generation units in distribution networks: an analytical approach. IEEE Trans Power Syst. 2018 May;33(3):2742–2753.

[21] Ehsan A, Yang Q. Optimal integration and planning of renewable distributed generation in the power distribution networks: A review of analytical techniques. Appl Energy. 2018 Jan;210:44–59.

[22] Gözel T, Hocaoglu MH. An analytical method for the sizing and siting of distributed generators in radial systems. Electr Power Syst. 2009 Jun;79(6):912–918.

[23] Hung DQ, Mithulananthan N, Lee KY. Optimal placement of dispatchable and nondispatchable renewable DG units in distribution networks for minimizing energy loss. Int J Electr Power Energy Syst. 2014 Feb;55:179–186.

[24] Selim A, Kamel S, Alghamdi AS, et al. Optimal placement of DGs in distribution system using an improved harris hawks optimizer based on single- and multi-objective approaches. IEEE Access. 2020;8:52815–52829.

[25] Kizito R, Li X, Sun K, et al. Optimal distributed generator placement in utility-based microgrids during a large-scale grid disturbance. IEEE Access. 2020;8:21333–21344.

[26] Hung DQ, Mithulananthan N, Bansal R. Analytical strategies for renewable distributed generation integration considering energy loss minimization. Appl Energy. 2013 May;105:75–85.

[27] Erdinc O, Tascikaraoglu A, Paterakis NG, et al. Comprehensive optimization model for sizing and siting of DG units, EV charging stations, and energy storage systems. IEEE Trans Smart Grid. 2018 Jul;9(4):3871–3882.

[28] Naderipour A, Nowdeh SA, Saftjani PB, et al. Deterministic and probabilistic multi-objective placement and sizing of wind renewable energy sources using improved spotted hyena optimizer. J Clean Prod. 2021 Mar;286:124941.

[29] Arasteh A, Alemi P, Beiraghi M. Optimal allocation of photovoltaic/wind energy system in distribution network using meta-heuristic algorithm. Appl Soft Comput. 2021 Sep;109:107594.

[30] Bazrafshan M, Gatsis N, Dallanese E. Placement and sizing of inverter-based renewable systems in multiphase distribution networks. IEEE Trans Power Syst. 2019 Mar;34(2):918–930.

[31] El-Ela AAA, El-Sehiemy RA, Abbas AS. Optimal placement and sizing of distributed generation and capacitor banks in distribution systems using water cycle algorithm. IEEE Syst J. 2018 Dec;12(4):3629–3636.

[32] Beskirli M, Koc I, Haklı H, et al. A new optimization algorithm for solving wind turbine placement problem: binary artificial algae algorithm. Renew Energy. 2018 Jun;121:301–308.

[33] Valencia A, Hincapie RA, Gallego RA. Optimal location, selection, and operation of battery energy storage systems and renewable distributed generation in medium-low voltage distribution networks. J Energy Storage. 2021 Feb;34(2020):102158.

[34] Fazliana Abdul Kadir A, Mohamed A, Shareef H, et al. An improved gravitational search algorithm for optimal placement and sizing of renewable distributed generation units in a distribution system for power quality enhancement. J Renew Sustain Energy. 2014 May;6(3):033112.

[35] Ibrahim K, Sirjani R, Shareef H. Performance assessment of pareto and non-pareto approaches for the optimal allocation of DG and DSTATCOM in the distribution system. Tehnicki Vjesnik. 2020 Oct;27(5):1654–1661.

[36] Ma C, Dasenbrock J, Töbermann JC, et al. A novel indicator for evaluation of the impact of distributed generations on the energy losses of low voltage distribution grids. Appl Energy. 2019 May;242:674–683.

[37] Ishak R, Mohamed A, Abdalla AN, et al. Optimal placement and sizing of distributed generators based on a novel MPSI index. Int J Electr Power Energy Syst. 2014 Sep;60:389–398.

[38] Memarzadeh G, Keynia F. A new index-based method for optimal DG placement in distribution networks. Eng Rep. 2020 Oct;2(10):1–15.

[39] Hassan AS, Othman EA, Bendary FM, et al. Optimal integration of distributed generation resources in active distribution networks for techno-economic benefits. Energy Rep. 2020 Nov;6:3462–3471.

[40] Li Z, Xu Y, Fang S, et al. Optimal placement of heterogeneous distributed generators in a grid-connected multi-energy microgrid under uncertainties. IET Renew Power Gener. 2019 Oct;13(14):2623–2633.

[41] Strunz K, Abbasi E, Abbey C, et al. Benchmark systems for network integration of renewable and distributed energy resources. CIGRE; 2014. (Tech. Rep.).

[42] Dolatabadi SH, Ghorbanian M, Siano P, et al. An enhanced IEEE 33 bus benchmark test system for distribution system studies. IEEE Trans Power Syst. 2021 May;36(3):2565–2572.